ELSEVIER

Materials Science and Engineering A289 (2000) 265–275

MATERIALS SCIENCE & ENGINEERING A

www.elsevier.com/locate/msea

Understanding the creep behavior of a 2.5D C_f–SiC composite II. Experimental specifications and macroscopic mechanical creep responses

G. Boitier, J.L. Chermant *, J. Vicens

Laboratoire d'Etudes et de Recherches sur les Matériaux, LERMAT, URA CNRS 1317 ISMRA, 6 Boulevard Maréchal Juin, 14050 Caen Cedex, France

Received 22 February 1999; received in revised form 22 February 2000

Abstract

Macroscopic results for a 2.5D C_f–SiC composite creep tested in tension are presented. After the development and the optimization of a new accurate high temperature tensile device, tests were conducted in argon, under a reduced pressure, for stresses ranging from 110 to 220 MPa and temperatures between 1273 and 1673 K. The macroscopic mechanical creep responses of the composite were analyzed and interpreted. Since ceramic matrix composites (CMCs) contain constituents of a different nature, with an influence of a structural aspect, it is not possible to apply the hypotheses of homogeneity and isotropy as described in Dorn's theory. Consequently, the physical meaning of the mechanical parameters, obtained by such a classical treatment, is limited. It is then necessary to discuss the global creep responses using an approach based on damage mechanics, which is more consistent with the specific features of the CMCs. This new approach adopted here reveals less classical parameters to be more accurate indicators of the creep behavior and the strain mechanisms of the 2.5D C_f–SiC composite. © 2000 Published by Elsevier Science S.A.

Keywords: 2.5D C_f–SiC composite; Creep curves; Dorn's formalism; Damage mechanics

1. Introduction

The creep behavior of monolithic ceramics has been extensively investigated whereas only few data from the literature are available concerning ceramic matrix composites (CMCs) with a monolithic ceramic matrix, in a large domain of temperatures and stresses [1–10]. This is due, on the one hand, to the recent development of that class of materials and, on the other hand, to the technological difficulties encountered in the development of accurate and reliable high temperature experiments [11–16].

In fact whatever the experimental device is, its development and optimization is a time-consuming exercise, especially in the case of high temperature mechanical devices where numerous and combined sensitive parameters are involved while they are most often not enough stable.

Nevertheless, the stress fields supported by CMC parts in service require creep tests to be performed, in order to determine their time to failure and to predict their lifetime.

The morphology and the microstructure of the 2.5D C_f–SiC composite investigated here has been previously described [17]. In this second paper, the tensile creep results obtained for this 2.5D C_f–SiC composite are presented, both through a classical approach and from the damage mechanics point of view, after some considerations about high temperature mechanical tests.

However, such mechanical responses only reveal the macroscopic aspect of the creep behavior of the material. Therefore, microstructural investigations have to be conducted at different scales to fully understand the mechanisms responsible for such responses. This will be discussed in a third paper [18].

* Corresponding author. Tel.: +33-2-31452664; fax: +33-2-31452660.

0921-5093/00/$ - see front matter © 2000 Published by Elsevier Science S.A.
PII: S0921-5093(00)00922-9

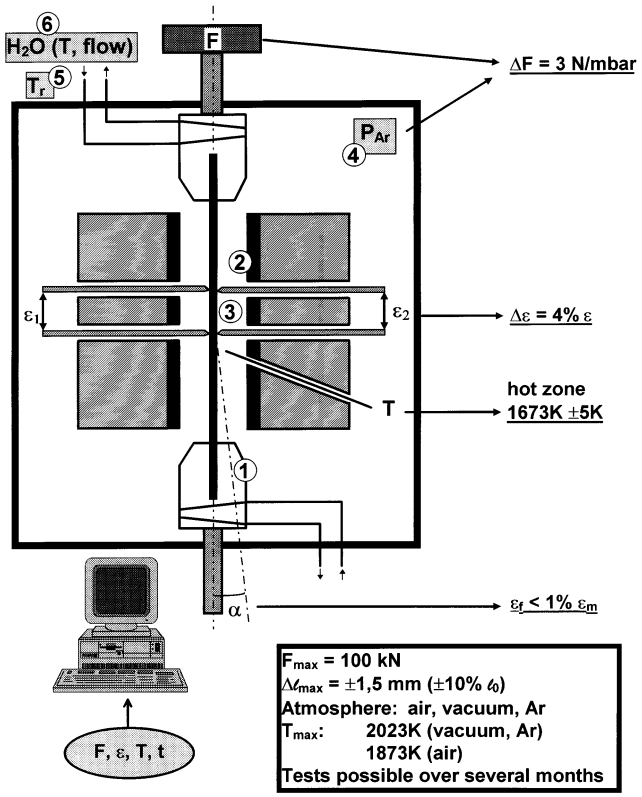

Fig. 1. Schematic drawing of our high temperature mechanical testing device (six major critical points are indicated).

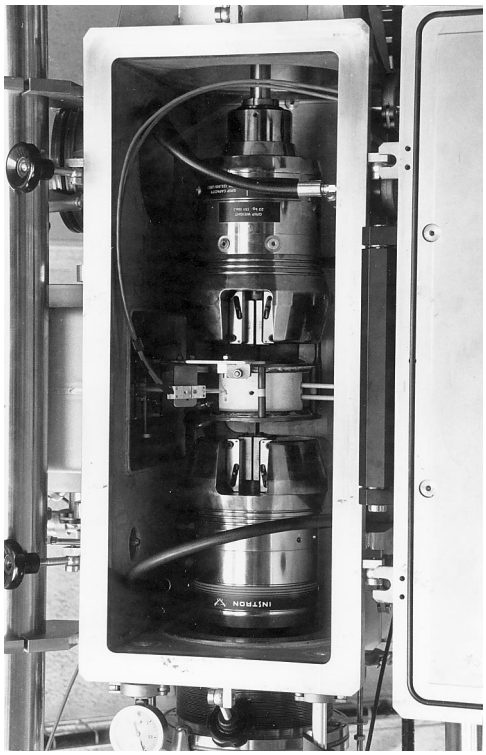

Fig. 2. Photograph of the experimental device developed in our laboratory with a detailed view of the grips, the furnace and the extensometers.

2. Experimental specifications for high temperature mechanical tests

An accurate analysis of the literature concerning creep tests at high temperatures in the case of ceramics or some ceramic matrix composites reveals that, even for tests performed in the same experimental conditions (temperature, stress, environment, same method of strain measurement (laser extensometry for example)), an absence of secondary stage is sometimes observed and a great spread in the strains and times to rupture (see for example Refs. [7,19–21]). For example, in the case of Si_3N_4 (SN88), the measured strains can vary up to 75% and the times to rupture up to 250% [21]. Such a dispersion cannot be only due to the inhomogeneity of these materials (inhomogeneous distribution and size of defects, …) and a lack of accuracy as well as experimental errors can be suspected. Then a comparison between such results appears to be impossible, as careless measurements can be far from the true values of both temperature and strain.

Once the load frame is chosen (most often an hydraulic one to avoid, for example, the play of the screws of the columns), and also the complete devices required for high temperature tests and measurements, many experimental parameters must be taken into consideration, especially regarding the load alignment ①, the furnace ②, the extensometer ③, the pressure of the test chamber ④, the room-temperature ⑤ and the flow and temperature of the cooling water ⑥ (Fig. 1). The following points appear, from our point of view, as very important [11–16]:

1. all the test specimens must be machined in the same conditions — shape, size, speed and rate of grinding, state of surface (roughness), … — the quality and reproducibility of the specimen machining have to be very high,
2. the load alignment is, from the advise of the most part of serious experts, one of the most important point to solve: the parasitic bending force must be avoided; it is absolutely necessary to use an instrumented specimen,
3. the materials of the furnace and of the susceptor must be chemically stable and inert regarding the test temperatures, the imposed atmospheres and the materials to be tested; they have to be as less volatile as possible to do not affect the mechanical behavior; let us recall that in the case of SiC based CMCs, the refractory cement of the furnace and of their caps must be particularly stable: one has to avoid any decomposition able to release oxygen which can oxidize the tested specimen, lead to the presence of silica, to a possible degradation of the susceptor (specially when it is made of graphite) as well as the arms of the extensometers,

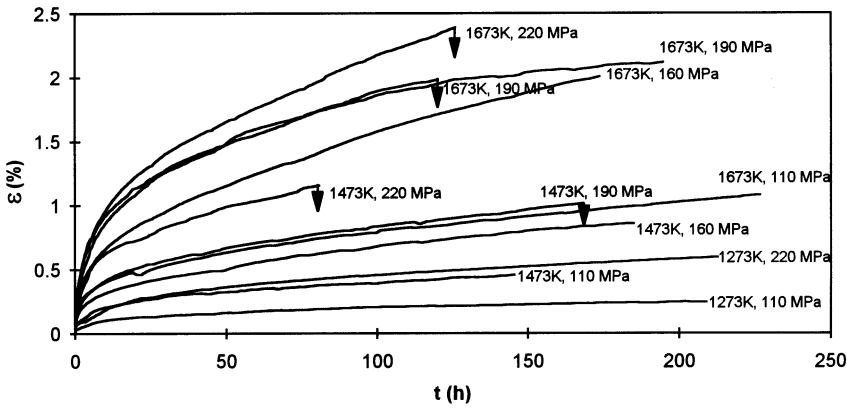

Fig. 3. Strain–time creep curves, ε–t, for the 2.5D C_f–SiC samples, tested under pure argon (vertical arrows indicate failure).

4. the choice of the type of thermocouple — PtRh or WRe — is also important. It is necessary to do not forget that platinum reacts at high temperature with silicon and their compounds [22,23]. The WRe thermocouples cannot be used for long-term tests as they react rapidly with O_2, N_2, C, after some hours at temperature higher than 1500 K, and so a thermocouple drift arises. Ta, Mo or W sheaths for thermocouples can be a solution, but the sheath can also react (!), and they are sometimes very brittle after use (that is specially the case for W). All the thermocouples are sensitive to the magnetic field induced in the RF coils and can play on the regulation stability; then the read value is lower than the true value. It follows that for the temperature measurement with a thermocouple we have to choose a compromise between the stability of the measurement with Pt thermocouples and the shift with WRe thermocouples.

Based on our long experience on high temperature mechanical tests, many precautions which have to be undertaken to properly determine mechanical responses are listed hereafter. One have to choose a correct position for the thermocouple to have a measurement of the true temperature of the specimen and not of the specimen environment. For tests performed at temperature higher than 1600 K, optical pyrometry is the best way to have a correct information on the temperature if the system is located far from the hot zone (to avoid any effect (coating, …) on the quartz window). The hot zone homogeneous in temperature must be perfectly known in the gauge of the test specimen where the strain measurement is made: that requires a correct thermal cartography of the furnace at the different test temperatures. The measurement of the true strain remains always extremely delicate; even if the laser extensometers are attractive, they are no more precise than capacitive or inductive mechanical extensometers. When strain measurement is performed with a laser extensometer, it requires a fixed flag/specimen connection, non-reactive, a rigorous parallelism between the two flags of the extensometer, no sliding during the tests [24], no vibration; moreover the changes in the refractive index of the hot atmosphere must be also taken into account, … The linearity of the response of any mechanical extensometer must always be verified. To avoid parasitic bending, the contact load on the mechanical extensometer arms must be limited; the best solution is to use two mechanical extensometers in opposition. A particular attention must be drawn to the extensometer arms — their chemical inertia regarding the tested material, the zones in contact (a point or a knife) — to the accuracy of the gauge length. The water temperature and flow for the cooling parts must be as constant as possible and these points are not so easy to solve (!); for example an increase of 1° of the cooling water can lead to an increase of several microns of deformation due only to a thermal expansion effect [15,25]. It is better to perform long-term tests in air-conditioned rooms. If the load cell is not in the airtight fence, the change in the pressure variation in the fence must be under control [26]. The electronic devices for the different types of measurements must be very stable as a function of time, on several months or even years.

Table 1
Mean duration of the different creep tests, t, and the corresponding maximum strains, ε, and creep rate, $\dot{\varepsilon}$, as a function of the experimental conditions for 2.5D C_f–SiC composite specimens

T (K)	σ (MPa)	t (h)	ε (%)	$\dot{\varepsilon}$ (s^{-1})	Rupture
1273	110	212	0.3	2.0×10^{-9}	No
	220	212	0.6	4.3×10^{-9}	No
1473	110	145	0.4	3.5×10^{-9}	No
	160	186	0.9	7.0×10^{-9}	No
	190	169	1.0	8.5×10^{-9}	Yes
	220	82	1.2	1.4×10^{-8}	Yes
1673	110	226	1.1	8.0×10^{-9}	No
	160	174	2.0	1.9×10^{-8}	No
	190	196	2.1	2.0×10^{-8}	No
	190	121	2.0	2.0×10^{-8}	Yes
	220	127	2.4	2.8×10^{-8}	Yes

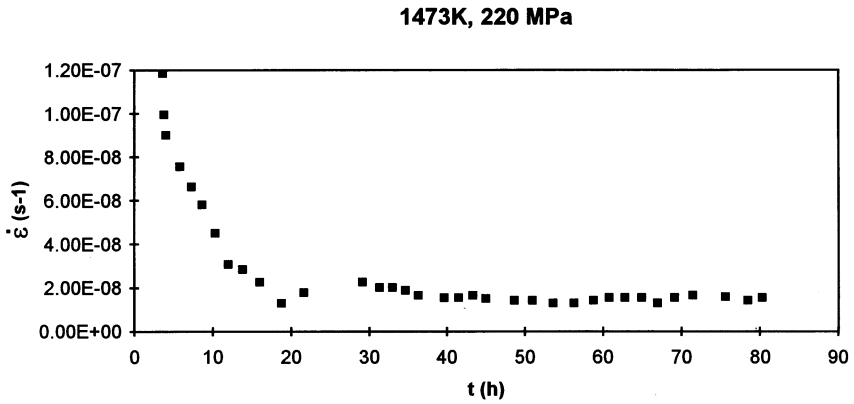

Fig. 4. Strain rate–time curve, $\dot{\varepsilon} - t$, for a 2.5D C_f–SiC specimen, tested under pure argon, at 1473 K, under 220 MPa.

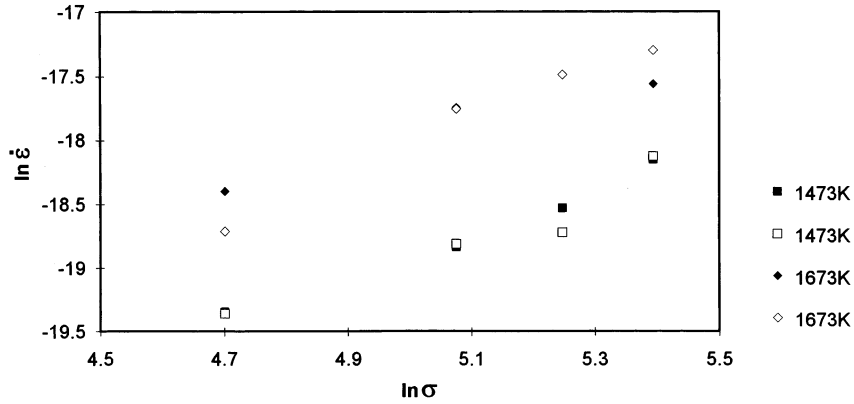

Fig. 5. Classical $\ln \dot{\varepsilon} - \ln \sigma$ curves for the 2.5D C_f–SiC samples, tested at 1473 and 1673 K (the open and closed symbols correspond to the values obtained via the two extensometers).

Moreover, in addition to these different technical problems to control with a lot of precautions, some other experimental effects must also be taken into account, such as the loading rate [27], the test protocol, some chemical decomposition and stability of materials utilized in the hot zone.

3. Experimental procedure

Our creep tests were performed with an hydraulic machine (Hydropuls PSB 100, Schenck, Darmstadt, Germany), with a load cell of 100 kN, and cooled grips with an hydraulic clamping (series 2742, Instron, Bucks, UK), a HF furnace (Célès, Lautenbach, France) with a graphite susceptor, working in a partial pressure of argon (50 mbar). An airtight cell (AET, Meylan, France) was added to the device to allow tests under various environments (2023 K under vacuum or argon). Two thermocouples W–Re 5%/W–Re 26% (Thermocoax, Suresnes, France) in a tantalum tube are used for the thermal regulation and lecture, together with an optical pyrometer (Mirage, Ircon, Niles, USA). The strain is measured via two resistive extensometers (DSA 15/10 HF, Schenck, Darmstadt, Germany) with SiC arms. A primary vacuum pump (E2M-18, Edwards, Cramley, UK) is used to empty the furnace (Fig. 2), before the filling by a partial pressure of pure argon (50 mbar).

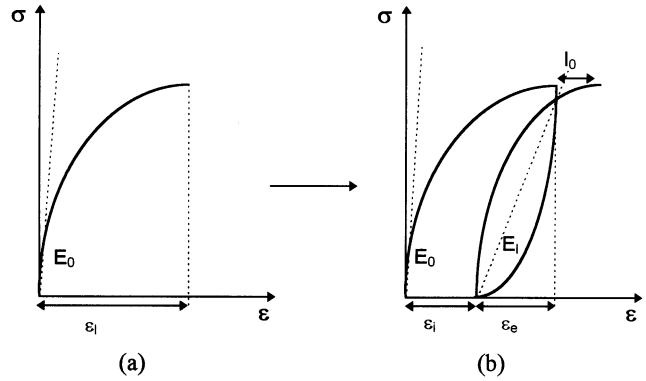

Fig. 6. Theoretical stress–strain, $\sigma - \varepsilon$, loading curves, illustrating the meaning of various mechanical parameters: ε_i, the loading strain; E_0, the initial elastic modulus; ε_i, the inelastic strain; ε_e, the elastic strain; E_l, the elastic modulus of the loaded material; l_0, the reloading mismatch.

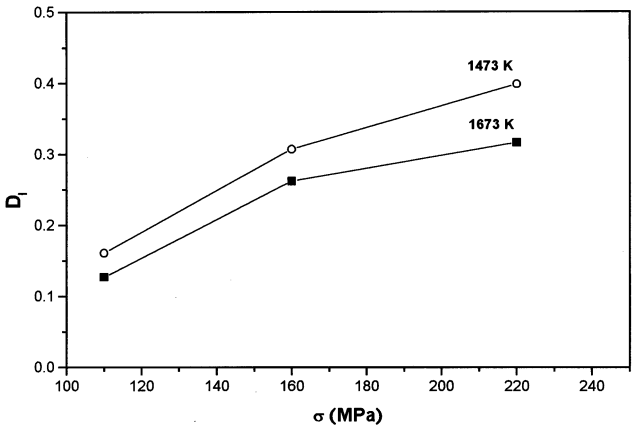

Fig. 7. Damage evolution upon loading at the beginning of the creep tests, as a function of the applied stress, D_I–σ.

Under these conditions, and taking care of the different points listed above, creep experiments were conducted between 1273 and 1673 K, and 110 and 220 MPa in the following experimental conditions: alignment: less than 2% of bending component; hot zone: length, 30 mm; stability, ± 1 K; measure, for example 1673 ± 15 K for the read temperature; strain, $\pm 1\%$.

4. Creep results

4.1. Strain–time curves (ε–t)

The strain–time curves, ε–t, obtained over the whole field of interest are gathered in Fig. 3. An almost noise-free shape is noticed for each one, which underlines the quality of the experiments conducted. The undulations and steps, mainly observed in the stationary stage, are due to unloading–reloading cycles performed periodically during creep tests. The purpose of such cycles will be discussed later.

Creep starts at a temperature as low as 1273 K even though the strain remains small ($\varepsilon = 0.6\%$ after 212 h under 220 MPa). When increasing temperature, for a given stress, the creep strain rises. Reciprocally, for a given temperature, the creep strain increases when rising stress. Nevertheless, in our field of investigation, the 2.5D C_f–SiC composite can stand the same stress levels at 1673 K as at 1273 K, which was not the case for 2D SiC_f–SiC composites, as Abbé has shown a significant drop of the maximum stress bearable when increasing temperature [1].

However, at 1473 and 1673 K, the higher tested stresses (i.e. 190 and 220 MPa) lead to the failure of the specimens. At 1473 K, under 220 MPa, the rupture

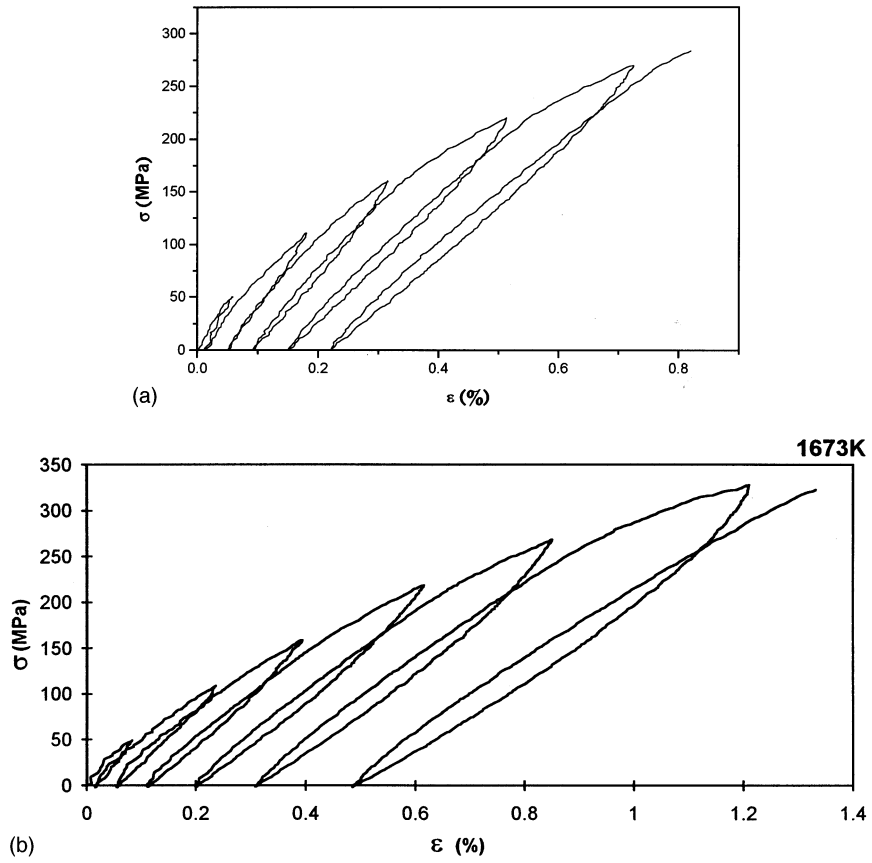

Fig. 8. Step-loading curves, under argon, for 2.5D C_f–SiC samples, tested at 1473 K (a) and 1673 K (b).

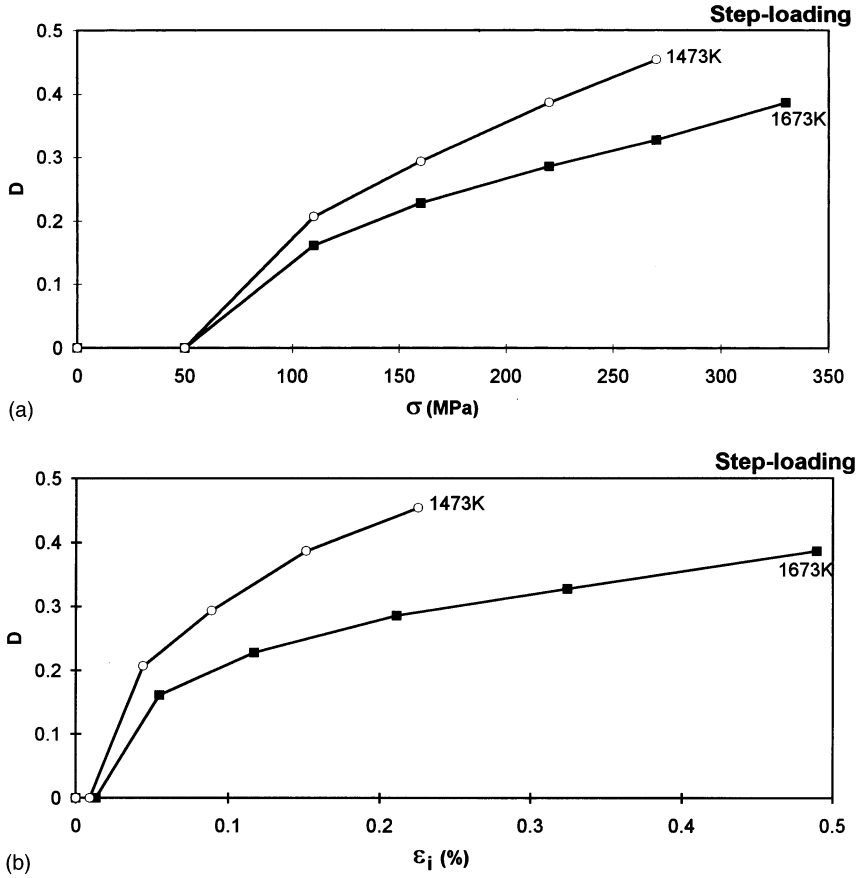

Fig. 9. Damage evolution upon tensile step-loading tests, D, as a function of either the applied stress, σ, (a) or the inelastic strain, ε_i, (b).

occurs within 82 h for a final creep strain of 1.2%. Under 190 MPa, the time to failure rises up to 169 h for a final creep strain of 1.0% (Table 1).

At 1673 K, under 220 MPa, the fracture of the specimen takes place after 128 h for a final creep strain of 2.4%. Under 190 MPa, an early failure is encountered after 121 h for a creep strain of 2.0% whereas other tests performed in the same conditions have been conducted without rupture for almost 200 h. All test parameters are gathered in Table 1.

Regarding the general aspect of the strain–time curves a transient creep stage is observed followed by a steady state. But, even for tests conducted until rupture, no tertiary stage has ever been obtained, as previously mentioned by Holmes and Morris for a 3D C_f–SiC composite [3].

4.2. Strain rate–strain curves ($\dot{\varepsilon} - \varepsilon$)

To determine more precisely the occurrence of the successive stages the strain rate–strain (or time) curves are useful. In fact, the stationary stage is of crucial importance as it corresponds to a domain of stable deformation of the specimen, with a minimum strain rate, before its catastrophic failure. However, in some specific cases, some authors have reported not to have ever observed such a steady state (see for example Ref. [7]). Nevertheless, such a particular behavior may be attributed to a real anomalous behavior of the batches of CMCs as well as to a lack of accuracy of the experimental device, or a careless handling of the experimenters.

Only one $\dot{\varepsilon} - \varepsilon$ curve is presented in Fig. 4, as an example, for a creep test conducted at 1473 K under 220 MPa. The occurrence of a steady state is evidenced. The strain rates measured in the stationary stage are displayed in Table 1. Globally, the strain rate range is between 2.0×10^{-9} (110 MPa, 1273 K) and 2.8×10^{-8} s^{-1} (220 MPa, 1673 K).

4.3. Stress exponent (n) and activation energy (Q)

The usual treatment of the creep data is done according to a classical formalism, defined for homogeneous and isotropic materials, known as Dorn's equation:

$$\dot{\varepsilon}_{ss} = A\sigma^n \exp\left(\frac{-Q}{RT}\right) \quad (1)$$

where $\dot{\varepsilon}_{ss}$ is the mean strain rate in the steady state, A is a constant, σ is the applied stress, n is the stress exponent, Q is the activation energy, R is the gas constant, and T is the temperature.

Using such a formalism, one can determine the values of the stress exponent and the activation energy, which refer to a given creep mechanism [28,29]. At constant temperature, the stress exponent is obtained as the slope of the $\ln \dot{\varepsilon} - \ln \sigma$ plot. The plots presented in Fig. 5 correspond to the tests performed at 1473 and 1673 K. At both temperatures, a linear relationship is obtained with almost the same slope. Therefore, the stress exponent calculated is close to 2. This seems to testify that, in our fields of stress and temperature, only one strain regime is encountered.

For a given stress, the value of the activation energy of the activated process is obtained through an Arrhenius plot, $\ln \dot{\varepsilon} - 1/T$. Whether the stress level is high (220 MPa) or low (110 MPa), the activation energy calculated is in the same order of magnitude: 80 and 60 kJ mol^{-1}, respectively for 220 and 110 MPa.

5. Discussion

The treatment of the macroscopic mechanical creep response of this 2.5D C_f–SiC composite, through a classical approach, based on Dorn's formalism, tends to prove the occurrence of only one strain mechanism whatever the stress and the temperature are [30,31]. In our field of investigation, the stress exponent is 1.8–2 and the activation energy is 60–80 kJ mol^{-1}. However, these values are far from the ones corresponding to the creep mechanism of either the fiber (for high modulus carbon fibers — HM 3000 — $n = 7$–8.5; $Q = 1000$–1200 kJ mol^{-1} [32,33]) or the matrix (for CVD–SiC tested in compression $n = 2.3$–3.7; $Q = 175$ kJ mol^{-1} [34]). Therefore, it can be said that in our field of investigation, the creep mechanism for the whole 2.5D C_f–SiC composite is not controlled by the classical macroscopic creep of one of its constituents (i.e. either the carbon fibers or the silicon carbide matrix).

Moreover, these classical parameters (i.e. n and Q) are defined theoretically for isotropic and homogeneous materials. But, in the case of composite materials, such hypotheses are not applicable, due to the association of constituents of different nature and the presence of architecture effects. Then the physical meaning of n and Q appears suspicious. In other words, does the 2.5D C_f–SiC composite creep in the classical meaning of that word? Nevertheless, this classical formalism generates qualitative elements of comparison with previous studies. Thus, a more detailed analysis of the macroscopic mechanical creep responses has to be conducted, in

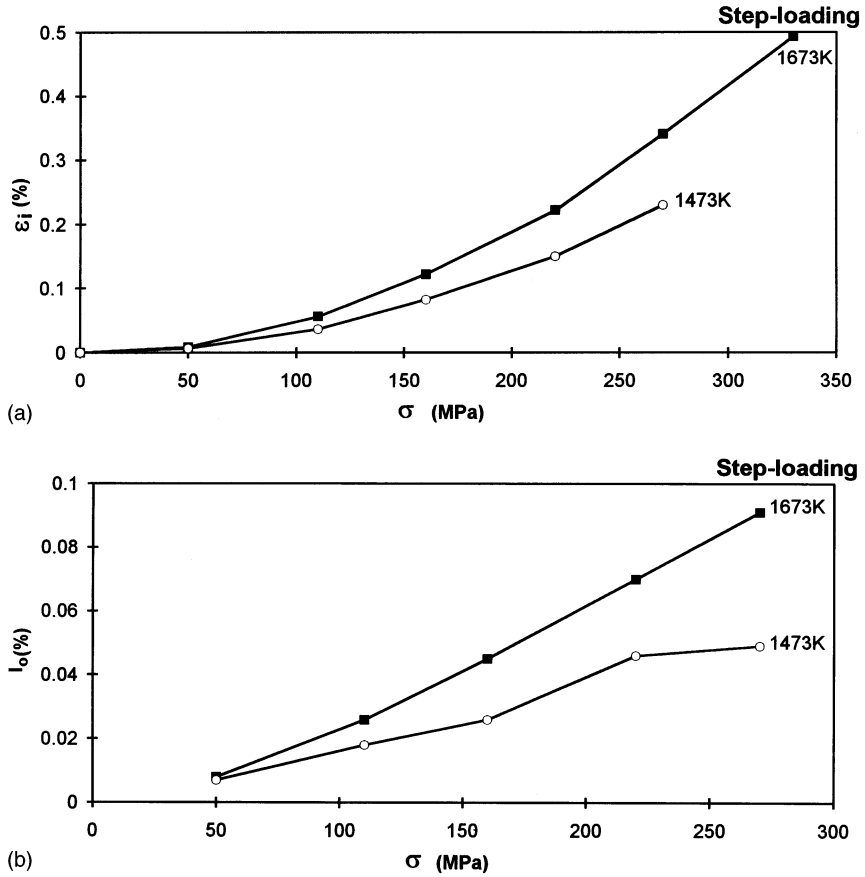

Fig. 10. Evolution of the inelastic strain, ε_i, (a) and of the reloading mismatch, l_0, (b) as functions of the applied stress, σ, due to tensile step–loading tests performed under argon, on 2.5D C_f–SiC specimens, at 1473 and 1673 K.

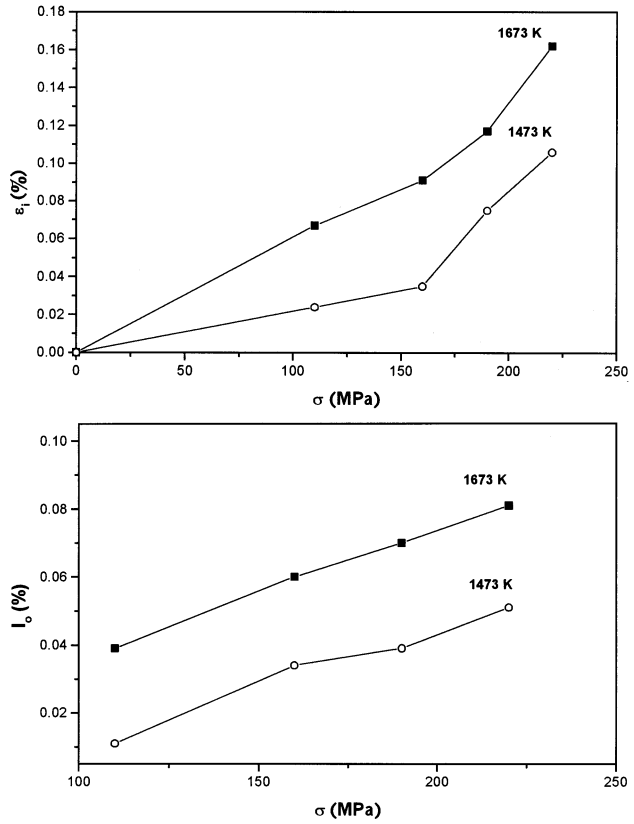

Fig. 11. Evolution of the inelastic strain, ε_i, (a) and of the reloading mismatch, l_0, (b) as functions of the applied stress, σ, due to the load application at the beginning the creep tests performed under argon, on 2.5D C_f–SiC specimens, at 1473 and 1673 K.

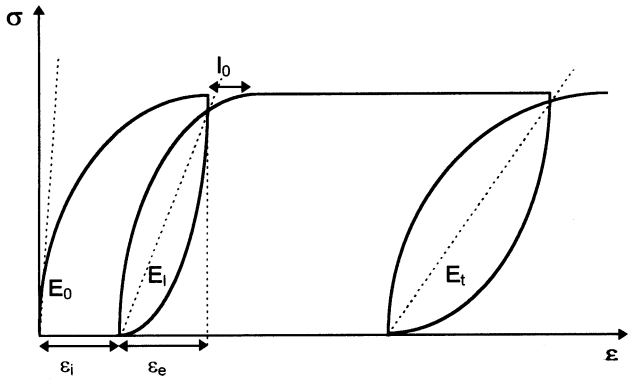

Fig. 12. Theoretical stress–strain curve, $\sigma-\varepsilon$, during a tensile creep test with unloading–reloading cycles.

order to obtain a deeper insight towards the creep mechanism of the composite, by taking into account its physico-chemical history [35].

Thus, a second approach has been attempted, based on step-loading tensile tests, in order to get a wider and richer palette of mechanical parameters, especially through the damage mechanism.

5.1. Influence of loading

The work of Maupas [25,36] has demonstrated the importance of the load application at the very beginning of any creep test on a 2D SiC_f–MLAS composite. First of all, it appears necessary to determine the influence of loading on the mechanical characteristics of the tested sample.

Through monotonous loading, only the loading strain, ε_l, and the initial elastic modulus, E_0, are available (Fig. 6a), which is quite limited. By making an unloading–reloading cycle, right after the load application, many other mechanical parameters are obtained as illustrated in Fig. 6b: the inelastic strain (ε_i) corresponding to the permanent strain after unloading, the elastic strain (ε_e) corresponding to the recovered strain upon unloading, the elastic modulus of the loaded material (E_l) and the reloading mismatch (l_0) corresponding to the gap between the strain at the end of loading and the strain at the end of reloading.

The influence of loading can be depicted through a damage parameter, D_l, as defined by Kachanov and Rabotnov [37,38]:

$$D_l = 1 - (E_l/E_0) \quad (2)$$

E_l and D_l are representative of the damage due to the load application and define the initial mechanical state of the material regarding its creep behavior. Therefore, after the load application at the beginning of each creep test, an unloading–reloading cycle has been performed. The damage evolution due to the load application, at both 1473 and 1673 K, is presented as a function of the applied stress (Fig. 7). It is remarkable that the damage increases as the stress increases and the temperature decreases.

5.2. Step-loading tensile tests

Considering the precedent result, and the shape of the loading curves, step-loading tensile tests were performed in order to follow the evolutions of E, ε_i, ε_e, l_0 and the damage parameter, D, as functions of load steps, at different temperatures.

The step-loading curves obtained at 1473 and 1673 K are presented in Fig. 8a and b. At both temperatures, each load induces a decrease of the elastic modulus which corresponds to a loss of stiffness of the material due to a damage accumulation. It can also be noticed that, for a same stress level, the hysteresis cycles are wider at 1673 than at 1473 K. The comparison between the two curves reveals a higher stiffness at 1473 than at 1673 K, which is confirmed by the damage curves in Fig. 9a and b. This underlines a more damageable behavior at 1473 K compared to 1673 K.

In parallel, an increase of the residual strains, ε_i, is observed at each step. In fact, for a same stress level,

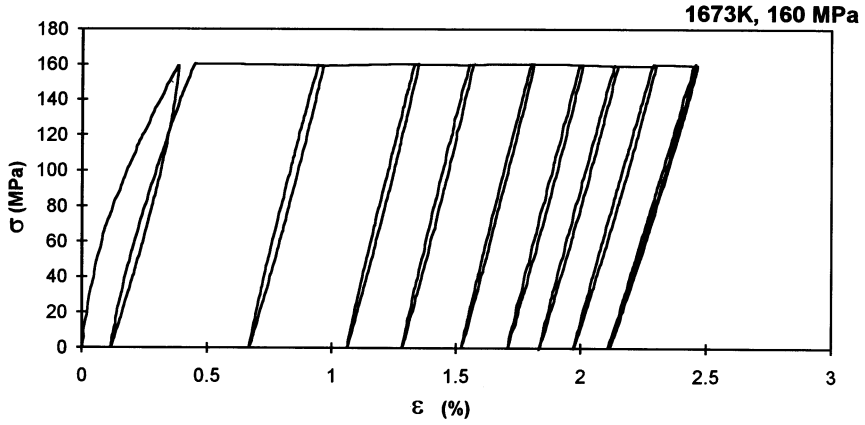

Fig. 13. Stress–strain curve, σ–ε, for a 2.5D C_f–SiC specimen creep tested under argon, at 1673 K, under 160 MPa, with unloading–reloading cycles.

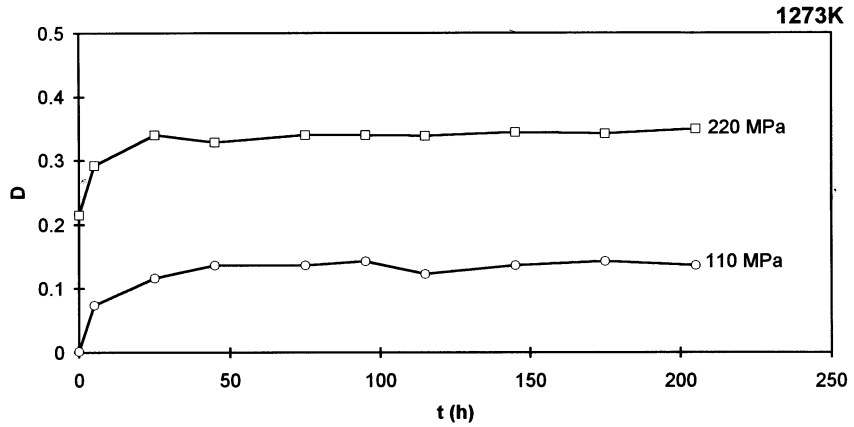

Fig. 14. Damage evolution as a function of time, D–t, for 2.5D C_f–SiC samples creep tested under argon, at 1273 K.

the associated inelastic strains are larger at 1673 than at 1473 K, as illustrated in Fig. 10a. This is in agreement with the work of Camus and Barbier for a 2D C_f–SiC composite [39]. Moreover, the reloading mismatch follows the same evolution upon stress and temperature as the inelastic strain (Fig. 10b). These results are distinctive features of a viscoplastic type mechanical behavior. This characteristic is more pronounced at 1673 K compared to 1473 K.

It is now possible to make a comparison between the monotonous loading curves and the step-loading curves. First, it has been established that each loading curve obtained at the beginning of a creep test fits the part of the envelope curve of the step loading curve to which it corresponds. Then, inelastic strains and reloading mismatches may be compared. The evolutions of ε_i and l_0, as functions of stress and temperature are comparable either in step loading or in monotonous loading (Figs. 10 and 11). But, for the highest stress levels, the inelastic strains, ε_i, are smaller upon monotonous loading whereas the reloading mismatches are larger. This can be attributed to a better stress redistribution upon step-loading. In fact, stress redistribution is a time-dependent mechanism. Therefore, at high stress levels, step loading tests give more time to the material to accommodate the stress, due to the presence of previous unloading–reloading cycles at lower stress levels.

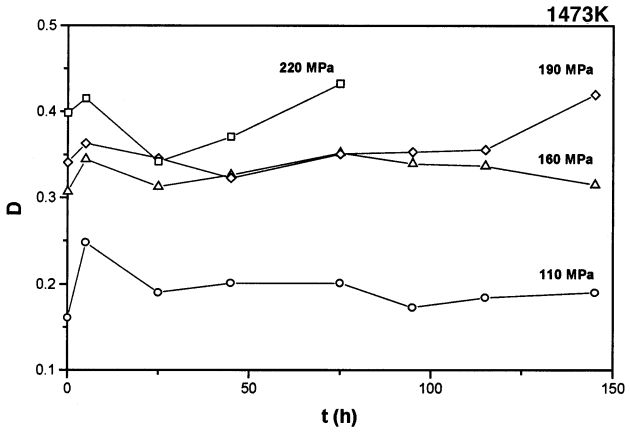

Fig. 15. Damage evolution as a function of time, D–t, for 2.5D C_f–SiC samples creep tested under argon, at 1473 K.

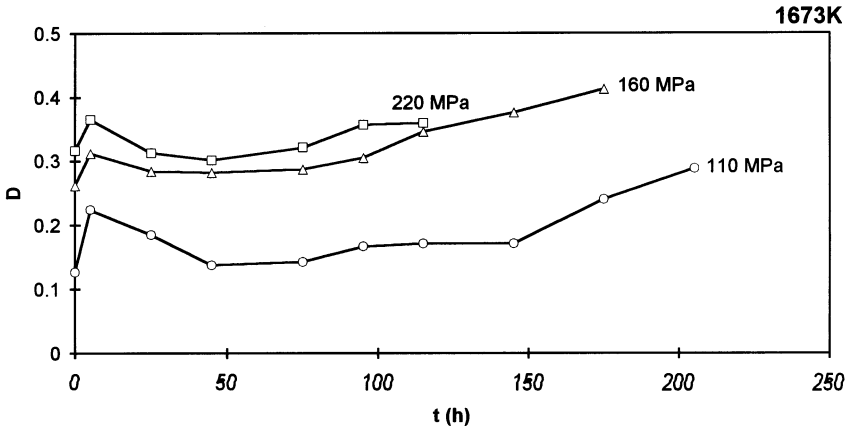

Fig. 16. Damage evolution as a function of time, $D-t$, for 2.5D C_f–SiC samples creep tested under argon, at 1673 K.

5.3. Damage and creep

Via step-loading tensile curves, different parameters are available as a function of a load increment. Such parameters are more accurate indicators of the material evolutions under loads, compared to monotonic loading. Thus, by making unloading–reloading cycles periodically during creep tests, it is possible to obtain the same type of parameters, no more as a function of a load increment but as a function of a time increment (Fig. 12). As an example, an experimental stress–strain curve, $\sigma-\varepsilon$, is presented in Fig. 13. One can notice that the cycles do not close upon reloading. Therefore, the same parameters as for step loading are now available regarding the creep behavior of the 2.5D C_f–SiC composite (i.e. E, ε_i, ε_e, l_0 and D).

As the cycles do not close upon reloading, the reloading mismatch has not been considered. Moreover, the evolutions of the inelastic strains do not bring new information in the discussion as they correspond to the creep strains added to the strains induced by the load application.

The most interesting parameter is the elastic strain as it gives the evolution of the elastic modulus through Hooke's law and consequently the damage parameter via Kachanov's equation [37]. At 1273 K, whatever the stress is, a damage accumulation is observed during the first 50 h of the creep experiments, followed by a stabilization (Fig. 14). At this temperature, damage is mainly accumulated during the transient creep stage. It can be also noticed that damage due to the load application is almost zero under 110 MPa while it becomes significant under 220 MPa.

At 1473 K, a damage accumulation is also evidenced in the very first hours of the creep tests but faster than at 1273 K (Fig. 15). This phenomenon is more pronounced when the applied load and the damage due to the load application are small. This first phase is then followed by a decrease of the damage parameter, which corresponds to the minima of the damage curves. Beyond that point the damage function remains almost steady under low stress conditions (i.e. 110 and 160 MPa), while it increases again under higher stress conditions (i.e. 190 and 220 MPa). The higher the stress, the higher and the faster this second damage accumulation is. At 1673 K, the damage function follows almost the same evolution as at 1473 K but, under all stress conditions, the second damage accumulation is always observed (Fig. 16). Nevertheless, for equivalent creep duration, the damage level reached at 1673 K is lower than at 1473 K. This confirms the more damageable behavior of the 2.5D C_f–SiC composite at 1473 K. This approach underlines the influence of the temperature on the damage. Moreover, it tends to demonstrate the existence of two creep strain regimes for the composite: one under low stress conditions, the other one under high stress levels. Nevertheless, the absence of a second damage increase under low stress conditions may be a consequence of the test duration being to short.

Based on the sole mechanical responses, the discussion cannot go any further, as the material has been only considered as a black box recorder. This clearly evidenced that a microstructural investigation of the tested materials is required to illustrate the mechanical investigation and to get a deeper interpretation of the particular shape of the damage curves and especially the damage apparent reduction. Thus, the ultimate step towards understanding the creep behavior will require a multiscale investigation from the macroscopic scale down to the nanometric one and will detailed in the following paper [18].

6. Conclusion

In this paper we have highlighted the limits of the Dorn's formalism when applied to composite materials with architecture effects, which ruin the hypotheses of

homogeneity and isotropy. However, regarding the creep rates obtained over the stress and temperature ranges, this classical approach demonstrates the good creep resistance of the 2.5D C_f–SiC composite.

Through a second approach, based on Kachanov's damage mechanics, more information have been extracted from the macroscopic creep responses of the material. As damage develops during creep tests, it can be said already that a damage-creep mechanism is responsible for the creep strain of the 2.5D C_f–SiC composite. A more damageable behavior has been evidenced at 1473 K whereas a more viscoplastic behavior has been found at 1673 K.

To fully understand the micromechanisms involved in this whole damage–creep mechanism and the subsequent creep behavior of the composite, a microstructural investigation has to be conducted at different scales [18].

Acknowledgements

The authors wish to thank SEP, Division de SNECMA (Le Haillan, St Médard en Jalles, France) and Région de Basse-Normandie for providing fellowship (G.B.). Drs D. Rouby, J.C. Sangleboeuf, J.P. Richard and F. Abbé are acknowledged for stimulating discussions. Special thanks are due to Mr H. Cubéro for its continuous and helpful contribution to the mechanical testing.

References

[1] F. Abbé, Fluage en flexion d'un composite SiC_f–SiC 2D, Thèse de Doctorat, University of Caen, France, 1990.
[2] J.W. Holmes, J. Mater. Sci. 26 (1991) 1808.
[3] J.W. Holmes, J. Morris, 15th Annual Conference on Ceramics and Advanced Composites, Cocoa Beach, FL, 1991.
[4] J.N. Adami, Comportement en fluage uniaxial sous vide d'un composite à matrice céramique bidirectionnel Al_2O_{3f}–SiC, Thèse de Doctorat ès Sciences Techniques, Ecole Polytechnique Fédérale of Zürich (Suisse), Institute for Advanced Materials, Commission of the European Communities, Petten, Pays-Bas, 1992.
[5] G.E. Hilmas, J.W. Holmes, R.T. Bhatt, J.A. DiCarlo, Ceram. Trans. 38 (1993) 291.
[6] N. Mozdzierz, M. Backhaus-Ricoult, J. Phys. IV C7 (1993) 1931.
[7] A.G. Evans, C. Weber, Mater. Sci. Eng. A208 (1996) 1.
[8] S. Zhu, M. Mizuno, Y. Kagawa, J. Cao, Y. Nagano, H. Kaya, Mater. Sci. Eng. A225 (1997) 69.
[9] S. Zhu, M. Mizuno, Y. Nagano, J. Cao, Y. Kagawa, H. Kaya, J. Am. Ceram. Soc. 81 (1998) 2269.
[10] T. Ishikawa, N. Suzuki, I.J. Davies, M. Shibuya, T. Hirokawa, J. Gotoh, in: High Temperature Ceramic Matrix Composites, HT-CMC3, CSJ Series, vol. 3, Publications of the Ceramic Society of Japan, Japan, 1999, p. 197.
[11] B.F. Dyson, R.D. Lohr, R. Morell, Mechanical Testing of Engineering Ceramics at High Temperatures, Elsevier Applied Science, Barking, UK, 1989.
[12] P. Han, Tensile Testing, ASM, Materials Park, 1992.
[13] R.D. Lohr, M. Steen, Ultra High Temperature Mechanical Testing, Woodhead, Cambridge, UK, 1995.
[14] F. Doreau, H. Maupas, H. Cubéro, J.L. Chermant, Rev. Intl. Htes. Temp. Réfract. 30 (1995) 1.
[15] G. Boitier, H. Maupas, H. Cubéro, J.L. Chermant, Rev. Comp. Mat. Av. 7 (1997) 143.
[16] G. Boitier, H. Cubéro, J.L. Chermant, in: High Temperature Ceramic Matrix Composites, HT-CMC3, CSJ Series, vol. 3, Publications of the Ceramic Society of Japan, Japan, 1999, p. 309.
[17] G. Boitier, J. Vicens, J.L. Chermant, Mater. Sci. Eng. A 279 (2000) 73.
[18] G. Boitier, J. Vicens, J.L. Chermant, Mater. Sci. Eng. A (2000) submitted.
[19] M.N. Menon, H.T. Fang, D.C. Wu, M.K. Ferber, K.L. More, C.L. Hubbard, T.A. Nolan, J. Am. Ceram. Soc. 77 (1994) 1217.
[20] C. Weber, K.T. Kim, F.E. Heredia, A.G. Evans, Mater. Sci. Eng. A196 (1995) 25.
[21] W.E. Luecke, S.M. Wiederhorn, J. Am. Ceram. Soc. 80 (1997) 831.
[22] R. Lacroix, Les Techniques de l'Ingénieur, R-2590, 1960.
[23] C.J. Morrison, in: R.D. Lohr, M. Steen (Eds.), Ultra High Temperature Mechanical Testing, Woodhead, Cambridge, UK, 1995, p. 128.
[24] W.E. Luecke, J.D. French, J. Am. Ceram. Soc. 79 (1996) 1617.
[25] H. Maupas, Fluage d'un composite SiC_f–MLAS 2D en flexion et en traction, Thèse de Doctorat, University of Caen, France, 1996.
[26] G. Boitier, Comportement en fluage et microstructure de composites C_f–SiC 2,5D, Thèse de Doctorat, University of Caen, France, 1997.
[27] B.F. Sørensen, J.W. Holmes, J. Am. Ceram. Soc. 79 (1996) 313.
[28] A.H. Chokshi, T.F. Langdon, Mat. Sci. Tech. 7 (1991) 577.
[29] S. Ogerby, B.F. Dyson, in: B. Wilshire, R.W. Evans (Eds.), Proceedings of the Fifth International Conference on Creep and Fracture of Engineering Materials and Structures, The Institute of Materials, London, 1993, p. 53.
[30] G. Boitier, J. Vicens, J.L. Chermant, in: J.C. Earthman, F.A. Mohamed (Eds.), Proceedings of the Seventh International Conference on Creep and Fracture of Engineering Materials and Structure, TMS, Warrendale, PA, 1997, p. 631.
[31] G. Boitier, J. Vicens, J.L. Chermant, in: A.M. Brandt V.C. Li, I.H. Marshall (Eds.), Proceedings of the Fifth International Symposium on Brittle Matrix Composites, BMC5, BIGRAF and Woodhead, Warsaw and Cambridge, UK, 1997, p. 507.
[32] G. Sines, Z. Yang, B.D. Vickers, Carbon 27 (1989) 403.
[33] K. Kogure, G. Sines, J.G. Lavin, Carbon 32 (1994) 715.
[34] C.H. Carter, R.F. Davis, J. Bentley, J. Am. Ceram. Soc. 67 (1984) 732.
[35] G. Boitier, J. Vicens, J.L. Chermant, J. Eur. Ceram. Soc. 18 (1998) 1835.
[36] H. Maupas, J.L. Chermant, Comp. Sci. Tech. 59 (1999) 19.
[37] L. Kachanov, Izv. Akad. Nauk SSR 8 (1958) 26.
[38] M. Rabotnov, Creep Problem in Structural Members, North-Holland, Amsterdam, 1989.
[39] G. Camus, J.E. Barbier, Ceram. Trans. 57 (1995) 407.